Analytical Spectrum Representation for Physical Waveform Optimization Requiring Extreme Fidelity

Charles A. Mohr, Shannon D. Blunt
Radar Systems Lab (RSL), University of Kansas, Lawrence, KS

***Abstract*—Optimization of physically realizable radar waveforms necessitates operating on a discretized representation that possesses sufficient fidelity, which can usually be achieved via adequate oversampling with respect to 3-dB bandwidth. However, it has been experimentally observed that the design of practical waveforms containing spectral notches requires an even higher degree of fidelity to achieve the low notch depths that may be needed for useful interference avoidance. Because such extreme fidelity translates into very high dimensionality, here an alternative approach is explored that involves the analytical Fourier transform of polyphase-coded FM (PCFM) waveforms, the continuous-time model for which is readily amenable to optimization and physical emission by real radar systems. The cost function and iterative solution that arises from this formulation, which is denoted as Analytical Spectrum Notching (ASpeN), facilitates the design of waveforms that are implementable in arbitrary waveform generation (AWG) hardware without the need for further "notch depth compensation" after up-sampling. This property is confirmed through experimental evaluation using RF test equipment in a loopback configuration.**

Keywords—radar waveform design, waveform diversity, polyphase-coded FM, spectral notching, interference avoidance

I. INTRODUCTION

The PCFM waveform formulation [1] was conceived as a means to design and implement FM radar waveforms [2, 3], which are inherently amenable for high power transmission, by means of a compact coding structure that is conducive to optimization. Moreover, this implementation can be used to incorporate unavoidable transmitter distortion effects directly into the optimization process [4, 5]. The PCFM formulation has been shown to have great utility for a wide variety of waveform-diverse attributes/capabilities including the direct control of emission spectral containment [4, 6], the generation of complementary FM noise waveforms [7], higher-order PCFM implementations [8], waveform "over-coding" [9], a particular form of MIMO denoted as spatial modulation [10, 11], and a particular form of radar-embedded communication [12, 13].

The continuous signals produced by the implementation of PCFM waveforms on an AWG are high-fidelity representations of the analytical PCFM structure. However, the optimization of these physical signals necessitates operating on a discretized form of the continuous waveform. While it has been shown that sufficient "over-sampling" with respect to the waveform's 3-dB bandwidth goes a long way to ameliorate the aliasing that arises when discretizing this non-bandlimited signal (if pulsed), it still cannot be completely avoided. Thus, when extreme fidelity is required, such as in the case of spectral notching of transmit waveforms, additional processing may be needed to compensate for lost notch depth when the optimized waveform is up-sampled for subsequent loading onto the AWG [14].

To address this modeling limitation, the analytical Fourier transform of the continuous PCFM waveform model is derived so that a more compact discretized form can be employed. This analytical representation provides insight into the behavior and structure of PCFM waveforms and likewise serves as a framework within which to perform localized frequency optimization while more easily addressing aliasing effects. It is demonstrated experimentally that this approach realizes waveforms that provide exceedingly low notch depths without the need for computationally costly compensation (e.g. [15]).

II. THE ANALYTICAL PCFM SPECTRUM

The first-order, continuous-time PCFM waveform is defined as [1]

$$s(t\,;\mathbf{x}) = \exp\left\{ j\left(\int_0^t g(\tau) * \left[\sum_{n=1}^{N} \alpha_n \delta(\tau-(n-1)T_{\mathrm{p}}) \right] d\tau \right) \right\} \quad (1)$$
$$= \exp\{ j\phi(t) \},$$

where $\delta(t)$ is an impulse function, $g(t)$ is a shaping filter with time support on $[0, T_{\mathrm{p}}]$, the pulsewidth is $T = NT_{\mathrm{p}}$, and the sequence $\mathbf{x} = [\alpha_1\ \alpha_2 \cdots \alpha_N]^T$ contains the PCFM values that parameterize the physical waveform. Further, the phase $\phi(t)$ can be written in the more succinct form

$$\phi(t) = \sum_{n=1}^{N} b_n(t)\, \alpha_n \ , \quad (2)$$

for

$$b_n(t) = \int_0^t g(\tau-(n-1)T_{\mathrm{p}})\, d\tau \quad (3)$$

the temporal, phase-domain basis function corresponding to the nth code value α_n. In other words, the continuous PCFM phase can be written as a linear combination of N weighted basis functions whose shapes are determined by the shaping filter $g(t)$. Although $b_n(t)$ can take on many forms, such as higher-order PCFM [8] or Legendre polynomials [16], for first-order PCFM the commonly used rectangular shaping filter for $g(t)$ results in the time-shifted basis functions of (3) for which the first T_{p} interval of each is a ramp (and constant thereafter).

The previous PCFM-based waveform design approaches [1, 4 – 9], all of which fundamentally seek to determine the values in the parameterizing vector $\mathbf{x}$ to meet some prescribed goal, would discretize the resulting continuous signal in (1) with

This work was supported by the Office of Naval Research under Contract #N00014-16-C-2029. DISTRIBUTION STATEMENT A. Approved for Public Release.

sufficient over-sampling relative to 3-dB bandwidth to capture an adequate portion of the spectral roll-off region such that aliasing is kept to an acceptable degree. In contrast, here we examine the analytical spectrum of this continuous waveform structure. To do so, it is useful to first reformulate some aspects of this signal model.

In (1) the $\alpha_n \in [-\pi, +\pi]$ term represents the total phase change (in radians) over the nth time interval of extent T_p, which is convenient for a subsequent discretized representation. For an analytical perspective, however, it is more convenient to define the nth instantaneous radial frequency as $\bar{\alpha}_n$ such that the total phase change over this interval is $\alpha_n = T_\mathrm{p}\,\bar{\alpha}_n$, and by extension $\bar{\mathbf{x}} = [\bar{\alpha}_1\ \bar{\alpha}_2 \cdots \bar{\alpha}_N]^T$ and $\mathbf{x} = T_\mathrm{p}\,\bar{\mathbf{x}}$. Consequently, the waveform model of (1), under the stipulation that $g(t)$ is a rectangular shaping filter, can alternatively be expressed as

$$s(t, \bar{\mathbf{x}}) = \sum_{n=1}^{N} \mathrm{rect}\left(\frac{t - T_\mathrm{p}(n - 1/2)}{T_\mathrm{p}}\right) \times \exp\left(j\left[(\bar{\alpha}_n(t - T_\mathrm{p}(n-1)) + T_\mathrm{p}\sum_{k=1}^{n-1}\bar{\alpha}_k\right]\right) \tag{4}$$

where

$$\mathrm{rect}(t) = \begin{cases} 1 & |\,t\,| \,<\, 1/2 \\ 0 & \text{otherwise}. \end{cases} \tag{5}$$

In this form, the ramp resulting from the integration of $g(t)$ in (3) is captured by the $\bar{\alpha}_n t$ term in the exponential, with the summation over the previous $\bar{\alpha}_1 T_\mathrm{p}$ to $\bar{\alpha}_{n-1} T_\mathrm{p}$ terms ensuring phase continuity, which is necessary for spectral containment.

Taking the Fourier transform of the components of (4) by linearity therefore realizes

$$\mathcal{F}\{s(t; \bar{\mathbf{x}})\} = \sum_{n=1}^{N} \int_{T_\mathrm{p}(n-1)}^{T_\mathrm{p} n} \exp\left(j\left[(\bar{\alpha}_n(t - T_\mathrm{p}(n-1)) + T_\mathrm{p}\sum_{k=1}^{n-1}\bar{\alpha}_k\right]\right) \times \exp(-j2\pi f t)\, dt, \tag{6}$$

in which the integration limits correspond to the time support of each rect(•) function. It can then be shown that (6) can be manipulated into the form

$$S(f; \bar{\mathbf{x}}) = \sum_{n=1}^{N} T_\mathrm{p} \frac{\sin(\rho_n(f))}{\rho_n(f)} \times \exp\left(j\left[\rho_n(f) - (n-1)T_\mathrm{p} 2\pi f + T_\mathrm{p}\sum_{k=1}^{n-1}\bar{\alpha}_k\right]\right), \tag{7}$$

for the frequency-domain function

$$\rho_n(f) = \frac{T_\mathrm{p}}{2}(\bar{\alpha}_n - 2\pi f). \tag{8}$$

Examination of (7) and (8) reveals that the first-order PCFM analytical spectrum consists of a summation of frequency-shifted sinc functions, where the nth sinc function is shifted to the nth instantaneous frequency value $\bar{\alpha}_n$. Moreover, each sinc function is scaled by an exponential term that contains a summation of previous $\bar{\alpha}_n$ values, which serves as a memory component that preserves continuity of phase in the time domain.

It is important to note that for a traditional polyphase code constructed using delay-shifted rect(•) functions [2, 3], the frequency response is likewise comprised of a sum of sinc functions, albeit without either the frequency shifting attribute or the memory term found in (7). Consequently, traditional polyphase codes cannot achieve the good spectral containment that can be attained for PCFM waveforms (e.g. see experimental comparison in [1]).

This analytical form of the PCFM spectrum provides a supplement to waveform optimization when extreme fidelity is required for localized frequency regions, such as in the case of forming spectral notches [14] in which aliasing otherwise limits the achievable notch depth. Of course, manipulation of this analytical spectrum for the purpose of waveform optimization still requires that it be properly discretized in the frequency domain.

III. Discretizing the Analytical PCFM Spectrum

Given the continuous (in frequency) analytical PCFM spectrum, we wish to discretize it to facilitate manipulation of the corresponding time-domain waveform such that extreme fidelity is preserved (to constrain aliasing effects). The following discusses how (7) and (8) provides this discretized representation, albeit in a manner that can be far more compact than what is achieved in the time-domain when the focus is on a localized frequency region (i.e. a spectral notch).

By definition, a time-limited signal has an infinite absolute bandwidth. Accordingly, the only way to unambiguously represent the spectrum of the discretized version of such a signal is to use a theoretically infinite sampling rate, which is not physically meaningful. Consequently, the frequency response after discretization invariably contains some amount of aliasing within the passband of the waveform, regardless of any "over-sampling" relative to 3-dB bandwidth.

Observe, however, that the analytical representation in (7) and (8) can be viewed as the spectrum corresponding to an infinite sampling rate (since it is the Fourier transform of the continuous waveform model), and thus all frequencies are represented unambiguously (i.e. no aliasing). Further, while discretization is still required, this form provides an advantage due to the inherent duality of the Fourier transform.

Specifically, it is well known that a continuous-time signal $s(t)$ can be perfectly reconstructed from its sampled version if the corresponding sampling rate is at least twice the highest frequency content of the signal. For a pulsed, and thus non-bandlimited, signal this condition clearly cannot be met. However, a duality arrangement exists whereby the frequency domain representation $S(f)$ can be perfectly reconstructed from its sampled version if the frequency domain "sampling rate" is at least twice the highest "temporal content" (i.e. time support) of the signal. From a physical perspective this dual statement is not really meaningful, but from a mathematical standpoint it means the analytical PCFM spectrum can be truly Nyquist "sampled" for the purpose of waveform optimization without suffering from a loss in fidelity.

More explicitly, a discretized form of (7) can be written as the infinite length vector

$$S(f_m;\bar{\mathbf{x}}) = \sum_{n=1}^{N} T_{\mathrm{p}} \frac{\sin(\rho_n(f_m))}{\rho_n(f_m)} \times \exp\left(j\left[\rho_n(f_m) - (n-1)2\pi T_{\mathrm{p}} f_m + T_{\mathrm{p}} \sum_{k=1}^{n-1} \bar{\alpha}_k \right] \right), \tag{9}$$

where

$$f_m = m\,\Delta f \tag{10}$$

for integer index $-\infty \le m \le +\infty$. Perfect reconstruction can therefore be obtained if

$$\Delta f \le \frac{1}{2T}. \tag{11}$$

Taken at face value, (9)-(11) implies that truncation is necessary to obtain a finite number of terms with which to perform optimization (i.e. determine $\bar{\mathbf{x}}$), thereby resulting in the need for a sufficiently large number to constrain the degree of aliasing. However, since spectral notches are localized in frequency by definition, only that region needs to be considered. While doing so would require operation on the entire time-domain representation, this analytical frequency-domain representation alternatively facilitates addressing only the values of $S(f_m;\bar{\mathbf{x}})$ at the discrete frequencies in the local vicinity with a granularity based on (11). Further, the sidelobe degradation that tends to arise from any manner of waveform notching [17] is largely compensated by the use of FM noise waveforms that do not repeat, and thus benefit from incoherent combining of sidelobes [18].

IV. Localized Waveform Spectrum Optimization

Consider an arbitrary FM waveform $s(t,\bar{\mathbf{x}})$ that has been optimized to possess (or at least reasonably approximate) some desired spectral shape that has satisfactory spectral containment (i.e. acceptable roll-off). We wish to insert a spectral notch in some part of the band defined on frequency interval $[f_{\min}, f_{\max}]$, which in the context of (9) can be accomplished by posing the simple cost function

$$J = \sum_m \left| S(f_m;\bar{\mathbf{x}}) \right|^2, \tag{12}$$

where f_m discretizes this frequency interval according to (11). For the number of discretized values in this interval denoted as M, the minimization of (12) then serves to determine the modified values of $\bar{\mathbf{x}}$ for which the resulting continuous signal implemented via (1) contains a deep spectral notch over this frequency region. Due to the fact that *a*) this cost function is not readily amenable to closed-form solution and *b*) we want the modified $\bar{\mathbf{x}}$ to remain close to the previously optimized result, an iterative approach is a prudent choice.

Here a gradient-descent method is used to minimize (12), with the overall approach denoted as Analytical Spectrum Notching (ASpeN). In particular, heavy ball gradient-descent [19] has been found to be effective for parameterized FM waveform optimization [6,7]. This approach differs from standard steepest-descent, where the search direction is the negative of the current gradient, in that the heavy ball search direction also includes the previous search direction. Specifically, the update is performed as

$$\bar{\mathbf{x}}_{k+1} = \bar{\mathbf{x}}_k + \mu_k \mathbf{p}_k, \tag{13}$$

where μ_k is the step size and

$$\mathbf{p}_k = \begin{cases} -\boldsymbol{g}_0 & \text{when } k = 0 \\ -\boldsymbol{g}_k + \beta \mathbf{p}_{k-1} & \text{otherwise} \end{cases}$$

is the current search direction for $0 \le \beta \le 1$. The step size is chosen using a simple backtracking algorithm [20]. If $\mathbf{p}_k$ is found to be an ascent direction it is reset to the steepest descent direction $-\mathbf{g}_k$ for that iteration.

Using the chain rule it can be shown that the gradient of (12) with respect to $\bar{\mathbf{x}}$ is

$$\nabla_{\bar{\mathbf{x}}} J = 2\Re\left\{ \sum_m \left(\nabla_{\bar{\mathbf{x}}} S(f_m;\bar{\mathbf{x}}) \right)^* S(f_m;\bar{\mathbf{x}}) \right\}, \tag{14}$$

where $\Re\{\cdot\}$ extracts the real part of the argument and

$$\nabla_{\bar{\mathbf{x}}} S(f_m;\bar{\mathbf{x}}) = \begin{bmatrix} \dfrac{\partial S(f_m;\bar{\mathbf{x}})}{\partial \bar{\alpha}_1} \\ \vdots \\ \dfrac{\partial S(f_m;\bar{\mathbf{x}})}{\partial \bar{\alpha}_N} \end{bmatrix}. \tag{15}$$

Based on (9), the nth derivative in (15) is therefore

$$\begin{aligned} \frac{\partial S(f_m;\bar{\mathbf{x}})}{\partial \bar{\alpha}_n} = & \left[\frac{T_{\mathrm{p}}^2}{2} \left(\frac{\exp(j\rho_n(f_m))}{\rho_n(f_m)} - \frac{\sin(\rho_n(f_m))}{\rho_n{}^2(f_m)} \right) \right. \\ & \left. \times \exp\left(j\left[\rho_n(f_m) - (n-1)2\pi f_m T_{\mathrm{p}} + T_{\mathrm{p}} \sum_{k=1}^{n-1} \bar{\alpha}_k \right] \right) \right] \\ & + \left[jT_{\mathrm{p}}{}^2 \sum_{\ell=n+1}^{N} \frac{\sin(\rho_\ell(f_m))}{\rho_\ell(f_m)} \right. \\ & \left. \times \exp\left(j\left[\rho_\ell(f_m) - (\ell-1)2\pi f_m T_{\mathrm{p}} + T_{\mathrm{p}} \sum_{k=1}^{\ell-1} \bar{\alpha}_k \right] \right) \right]. \end{aligned} \tag{16}$$

V. Simulation Results

To illustrate the impact of aliasing on waveform design, we first compare the analytical spectrum to the discrete-time spectrum obtained when applying a fast Fourier transform (FFT) to discretized PCFM waveforms. The simulated performance of ASpeN described in Sect. IV is then compared to the previous physical waveform notching approach [14].

A. Analytical Spectrum vs. Aliased Spectrum

To assess the effect that aliasing has on discretized representations of continuous pulsed FM waveforms, consider the generation of 10,000 different PCFM waveforms using (1) in which $N = 300$ code values $\alpha_n = T_{\mathrm{p}} \bar{\alpha}_n$ for each waveform are independently drawn from a uniform random distribution on $[-\pi, +\pi]$. The analytical and FFT spectra, computed for each waveform, are then scaled relative to the bandwidth and pulse width T such that the same frequencies are aligned for

comparison. In Figs. 1 and 2, the mean power spectra of all 10,000 waveforms in each case is plotted.

In Fig. 1, an over-sampling factor of 3 relative to 3-dB bandwidth is used to determine the FFT spectrum and the analytical spectrum is the ground truth. While aliasing in the passband is rather small (on a dB scale), it is clear in the roll-off region that the FFT spectrum is indeed experiencing some notable aliasing effects, with nearly an order of magnitude difference at the edges of the figure. Also note that, with $N = 300$ and a factor of 3 over-sampling, the discretized vector to which the FFT is applied has a length of 900.

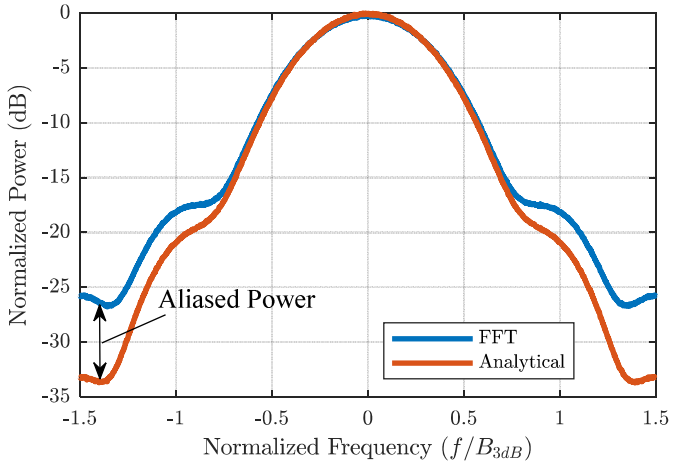

Fig. 1. The mean spectra of 10,000 randomly parameterized PCFM waveforms obtained via FFT and the analytical formulation. The FFT waveforms have an oversampling factor of 3.

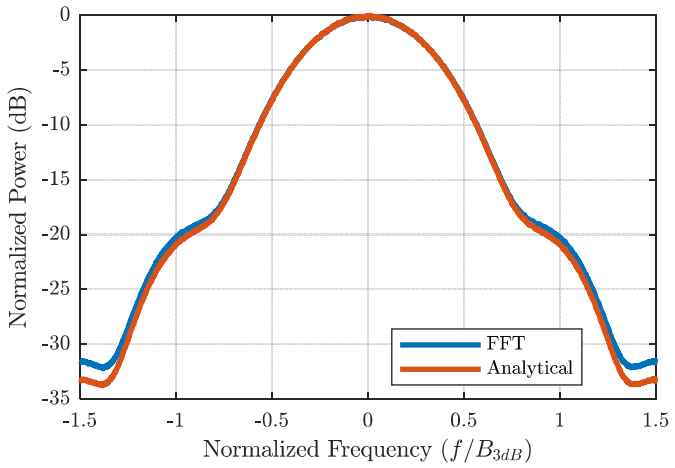

Fig. 2. The mean spectra of 10,000 randomly parameterized PCFM waveforms obtained via FFT and the analytical formulation. The FFT waveforms have an oversampling factor of 6.

From the perspective of the FFT spectrum, aliasing can be reduced by simply increasing the degree of over-sampling relative to the 3-dB bandwidth. For example, Fig. 2 shows that by increasing the over-sampling from 3 (in Fig. 1) to 6, the impact of aliasing is much reduced because the FFT is able to assign much of the previously aliased power to higher frequency bins (not shown). However, the length of the discretized vector for the FFT spectrum in Fig. 2 is now 1800.

Some key takeaways from these results are as follows. Only modest over-sampling relative to 3-dB bandwidth is needed to estimate the passband accurately. However, higher over-sampling is required to faithfully capture the lower power regions such as in the spectral roll-off. This effect is likewise observed for spectral notches because they are designed to have sufficient depth to avoid in-band interference. In the generation of physical notched waveforms [14] it has been observed that notches tend to get filled-in after a waveform is up-sampled for loading onto the AWG, which has necessitated "notch depth compensation" (or "re-notching") procedures that can be computationally expensive. It is next shown that notching based on the analytical spectrum allows this step to be avoided.

B. Analytical Spectrum Notching (ASpeN)

To assess the efficacy of the ASpeN procedure, two sets of 1000 optimized FM noise waveforms were produced. Both sets were first generated using the pseudo-random optimized FM (or PRO-FM) procedure from [18] which realizes a set of non-repeating (i.e. unique) waveforms that have a desired power spectrum via alternating time/frequency projections of independent random PCFM [1] initializations. Both sets of 1000 waveforms were designed to have a time-bandwidth product of $BT = 300$, with one set also having a stationary spectral notch that is approximately 10% of the 3-dB bandwidth.

It has been found that the PRO-FM waveform design process [18], despite involving a spectral shaping step, is not able to achieve a notch depth that would be considered adequate for most situations (a maximum of only about 20 dB has been observed). The previous approach to obtaining deeper notches for these waveforms [14], which is considered here for comparison purposes, is to apply the Reiterative Uniform Weighting Optimization (RUWO) algorithm [15] to each (shallowly notched) PRO-FM waveform. Because it involves the recursive application of a notching projection that has the same dimensionality as the discretized waveform, this approach is rather computationally costly, particularly for cognitive systems in which the latency incurred for waveform modifications may be the deciding factor in whether an approach is practically feasible [14]. Based on an over-sampling factor of 3 and BT of 300, the dimensionality for this RUWO implementation is 900.

For the purpose of employing the ASpeN procedure of Section IV, it is convenient that the discretized form of PRO-FM optimized waveforms (which are initialized with random PCFM) can likewise be well approximated as maximally over-coded PCFM waveforms [9]. This conversion is accomplished by unwrapping the phase, taking the element-wise difference over the discrete phase history, and then using these phase-change parameters as the α_n values in a first-order PCFM code. For the set of 1000 notch-free PRO-FM waveforms, ASpeN is applied to produce a notch in each that occurs in the same location as in the RUWO-generated set and with the same notch width (10% of the 3-dB bandwidth). Consequently, (10) and (11) dictate that $2(BT)(W_n) = 60$ analytical frequency values are needed to form a deep notch in this manner, where W_n is the width of the notch as a fraction of 3 dB bandwidth.

The mean spectrum is computed over each set of 1000 notched waveforms. Figure 3 illustrates these results when the

RUWO-modified mean spectrum is generated via FFT and the ASpeN-modified mean spectrum is produced via the analytical form in Sect. II (discretized to capture the same frequency interval). It is observed that the RUWO approach is able to produce a notch depth of roughly −60 dB while ASpeN realizes a much deeper notch of almost −80 dB.

At this point, an interesting observation can be made when the ASpeN-modified waveforms are likewise evaluated by discretizing applying an FFT to each. Figure 4 illustrates the result when the RUWO and ASpeN-modified mean spectra are presented in this way, with the latter now appearing to have lost more than 55 dB of notch depth. This dramatic difference (in appearance) is because the FFT-based spectrum incurs substantial aliasing, making the apparent notch much shallower. Of course, it is important to note that when the ASpeN-modified waveforms are generated at passband they still retain the original notch depth shown in Fig. 3.

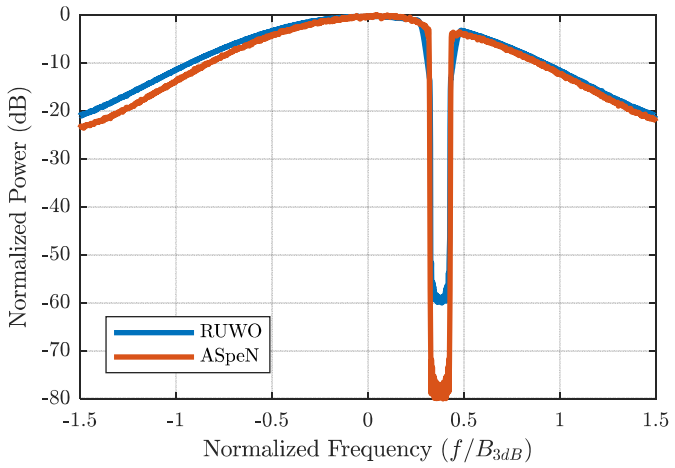

Fig. 3. Mean spectra of 1000 PRO-FM waveforms modified using ASpeN (plotting analytical spectrum) and RUWO (plotting FFT spectrum).

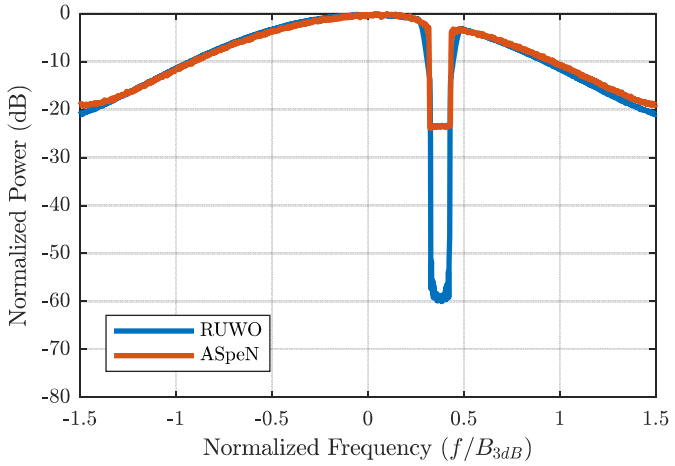

Fig. 4. Mean spectra of 1000 notched PRO-FM waveforms modified using ASpeN (plotting FFT spectrum) and RUWO (plotting FFT spectrum). The former now appears (falsely) to have a shallower notch due to aliasing.

VI. Experimental Results

To experimentally assess the performance of the analytical formulation, the ASpeN-modified and RUWO-modified notched waveform sets were each up-sampled by a factor of 50 from a baseband sampling rate of 200 MSamples/sec to 10 GSamples/sec, digitally up-converted to a center frequency of 3.55 GHz, implemented on a Tektronix AWG70002A having a 10-bit depth, and then captured in loopback on a Rhode & Schwarz FSW26 real-time spectrum analyzer (RSA) at a rate of 200 Msamples/sec. To emulate (at least partially) a realistic transmitter/receiver chain, the AWG-generated waveforms were routed through a class A amplifier and then an attenuator, before being passed through a low-noise amplifier (LNA) for subsequent capture by the RSA. Each $BT = 300$ waveform had a duration of $T = 4.5$ μs and a bandwidth of $B = 66.7$ MHz.

Figure 5 shows the mean spectra of the loopback captured versions of the two sets of waveforms from Fig. 3. The RUWO-modified waveforms experienced more than 30 dB degradation in notch depth (from −60 dB to a little above −30 dB). The ASpeN-modified waveforms experienced 23 dB of notch depth degradation, though since the notch was so much lower to begin with (−80 dB), the end result of −57 dB is nearly as good as the RUWO notch prior to physical implementation.

At this stage of waveform implementation, using a Class A (i.e. linear) amplifier, notch depth as low as −52 dB has also previously been observed [21]. However, that result, which is still 5 dB inferior to ASpeN, required the application of a "re-notching" procedure at passband, which incurs a rather high computational cost due to the very high sampling rate involved.

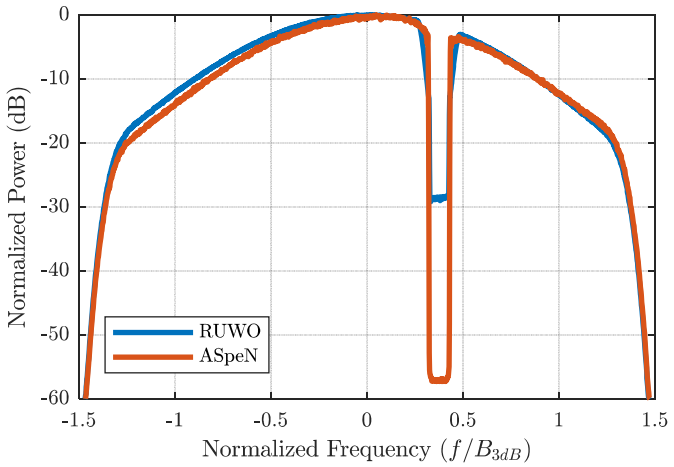

Fig. 5. Loopback captured mean spectra of 1000 PRO-FM waveforms formed using ASpeN and pre-notched RUWO (both are FFT spectra with oversampling factor of 6)

Finally, Fig. 6 shows the coherently integrated autocorrelations (i.e. zero Doppler response for Doppler processing) for each set of the loopback captured waveforms. While both cases demonstrate relatively low range sidelobes due to the incoherent combining that arises whenever non-repeating random waveforms are used, the RUWO result is clearly superior to ASpeN in this instance. However, this difference is not due to the RUWO/ASpeN methods themselves, but is because the former employs tapering of the notch edges, which was shown in [21] to alleviate the $\sin(x)/x$

sidelobes that otherwise arise. Ongoing work is investigating how ASpeN can likewise incorporate notch tapering so that similar sidelobe suppression can be achieved..

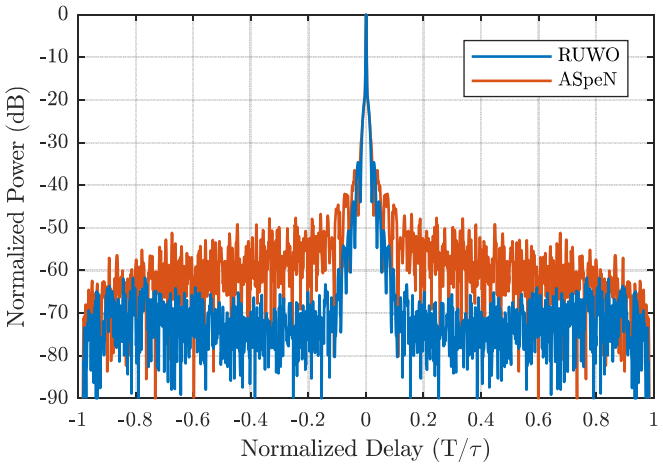

Fig. 6. Integrated autocorrelations of loopback captured versions of the ASpeN and RUWO modified PRO-FM waveforms

VII. Conclusions

The analytical Fourier transform of the first-order PCFM waveform implementation has been derived and shown to naturally address the aliasing effects inherent to sampling the time domain representation. This formulation was then used to develop the ASpeN method for notching of arbitrary FM waveforms which is capable of attaining excellent notch depth without requiring subsequent compensation after conversion to passband. Experimental loopback measurements confirm that the ASpeN method is viable in practice, with ongoing work exploring how notch tapering can also be incorporated.

References

[1] S.D. Blunt, M. Cook, J. Jakabosky, J.D. Graaf, E. Perrins, "Polyphase-coded FM (PCFM) radar waveforms, part I: implementation," *IEEE Trans. AES*, vol. 50, no. 3, pp. 2218–2229, July 2014.

[2] N. Levanon and E. Mozeson, *Radar Signals*, John Wiley & Sons, Inc., Hoboken, NJ, 2004.

[3] S.D. Blunt, E.L. Mokole, "An overview of radar waveform diversity," *IEEE AESS Systems Mag.*, vol. 31, no. 11, pp. 2-42, Nov. 2016.

[4] S.D. Blunt, J. Jakabosky, M. Cook, J. Stiles, S. Seguin, E.L. Mokole, "Polyphase-coded FM (PCFM) radar waveforms, part II: optimization," *IEEE Trans. AES*, vol. 50, no. 3, pp. 2230–2241, July 2014.

[5] J. Jakabosky, P. McCormick, S.D. Blunt, "Implementation & design of physical radar waveform diversity," *IEEE AESS Systems Mag*., vol. 31, no. 12, pp. 26-33, Dec. 2016.

[6] C.A. Mohr, P.M. McCormick, S.D. Blunt, C. Mott, "Spectrally-efficient FM noise radar waveforms optimized in the logarithmic domain," *IEEE Radar Conf*., Oklahoma City, OK, Apr. 2018.

[7] C.A. Mohr, P.M. McCormick, S.D. Blunt, "Optimized complementary waveform subsets within an FM noise radar CPI," *IEEE Radar Conf*., Oklahoma City, OK, Apr. 2018.

[8] P.S. Tan, J. Jakabosky, J.M. Stiles, S.D. Blunt, "On higher-order representations of polyphase-coded FM radar waveforms," *IEEE Intl. Radar Conf*., Arlington, VA, May 2015.

[9] J. Jakabosky, S. D. Blunt and B. Himed, "Optimization of "over-coded" radar waveforms," *IEEE Radar Conf*., Cincinnati, OH, May 2014.

[10] S.D. Blunt, P. McCormick, T. Higgins, M. Rangaswamy, "Physical emission of spatially-modulated radar," *IET Radar, Sonar & Navigation*, vol. 8, no. 12, pp. 1234-1246, Dec. 2014.

[11] G. Zook, P. McCormick, S.D. Blunt, "Fixational eye movement radar: random spatial modulation," *IEEE Radar Conf*., Oklahoma City, OK, Apr. 2018.

[12] C. Sahin, J. Jakabosky, P. McCormick, J. Metcalf, S. Blunt, "A novel approach for embedding communication symbols into physical radar waveforms," *IEEE Radar Conf*., Seattle, WA, May 2017.

[13] C. Sahin, J.G. Metcalf, A. Kordik, T. Kendo, T. Corigliano, "Experimental validation of phase-attached radar/communication (PARC) waveforms: radar performance," *IEEE Intl. Conf. Radar*, Brisbane, Australia, Aug. 2018.

[14] B. Ravenscroft, J.W. Owen, J. Jakabosky, S.D. Blunt, A.F. Martone, K.D. Sherbondy, "Experimental demonstration and analysis of cognitive spectrum sensing & notching," *IET Radar, Sonar & Navigation*, vol. 12, no. 12, pp. 1466-1475, Dec. 2018.

[15] T. Higgins, T. Webster A. K. Shackelford, "Mitigating interference via spatial and spectral nulls," *IET Intl. Conf. Radar Systems*, Glasgow, UK, Oct. 2012.

[16] P.M. McCormick, S.D. Blunt, "Gradient-based coded-FM waveform design using Legendre polynomials," *IET Intl. Conf. Radar Systems*, Belfast, UK, Oct. 2017.

[17] S.W. Frost, B. Rigling, "Sidelobe predictions for spectrally-disjoint radar waveforms," *IEEE Radar Conf*., May 2012.

[18] J. Jakabosky, S. D. Blunt, B. Himed, "Spectral-shape optimized FM noise radar for pulse agility," *IEEE Radar Conf*., Philadelphia, PA, May 2016.

[19] E. Ghadimi, R. Feyzmahdavian, M. Johansson, "Global convergence of the heavy-ball method for convex optimization," *European Control Conf*., Linz, Austria, July 2015.

[20] J. Nocedal, S. Wright, *Numerical Optimization*, Springer Science & Business Media, 2006.

[21] J. Jakabosky, B. Ravenscroft, S.D. Blunt, A. Martone, "Gapped spectrum shaping for tandem-hopped radar/communications & cognitive sensing," *IEEE Radar Conf*., Philadelphia, PA, May 2016.